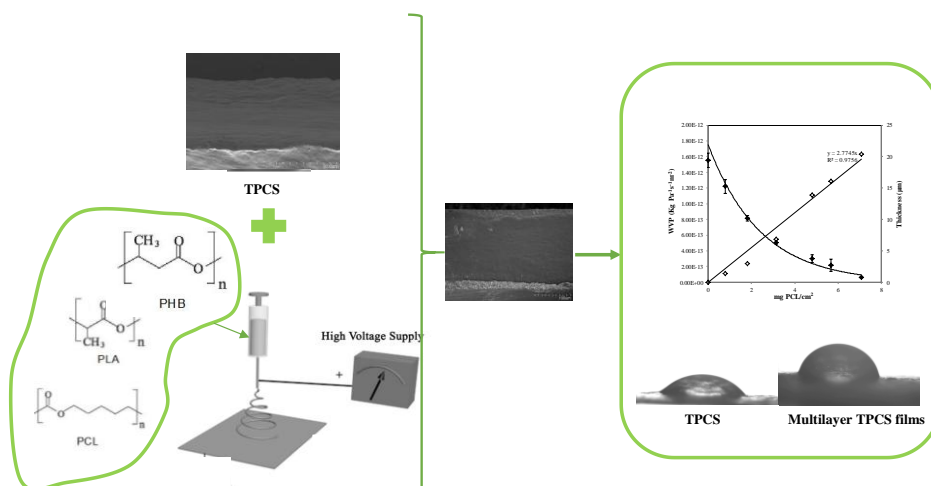


Graphical Abstract

Tailoring barrier properties of thermoplastic corn starch-based films (TPCS) by means of a multilayer design

María José Fabra*, Amparo López-Rubio, Luis Cabedo, Jose M. Lagaron



26 **Abstract**

27 This work compares the effect of adding different biopolyester electrospun coatings
28 made of polycaprolactone (PCL), polylactic acid (PLA) and polyhydroxybutyrate
29 (PHB) on oxygen and water vapour barrier properties of a thermoplastic corn starch
30 (TPCS) film. The morphology of the developed multilayer structures was also examined
31 by Scanning Electron Microscopy (SEM). Results showed a positive linear relationship
32 between the amount of the electrospun coatings deposited onto both sides of the TPCS
33 film and the thickness of the coating. Interestingly, the addition of electrospun
34 biopolyester coatings led to an exponential oxygen and water vapour permeability drop
35 as the amount of the electrospun coating increased. This study demonstrated the
36 versatility of the technology here proposed to tailor the barrier properties of food
37 packaging materials according to the final intended use.

38
39
40 **Keywords:** TPCS, Electrospinning, Multilayer, Barrier properties, Biopolyesters.

41

1
2
3
4
5
6
7
8
9
10
11
12
13
14
15
16
17
18
19
20
21
22
23
24
25
26
27
28
29
30
31
32
33
34
35
36
37
38
39
40
41
42
43
44
45
46
47
48
49
50
51
52
53
54
55
56
57
58
59
60
61
62
63
64
65

42 1. INTRODUCTION

43 The use of biopolymers has received increased attention in the last decades as potential
44 substitutes for conventional polymers in a broad range of applications. Among
45 biopolymers, polysaccharides, like starch, are interesting renewable resources that have
46 different applications. Indeed, the introduction of starch in the plastic sector has been
47 motivated by its low cost and biodegradability and by the fact that it is available in large
48 quantities (Xu *et al.*, 2005). However, starch cannot be processed through conventional
49 plastic equipment without further modification because its degradation begins at a
50 temperature lower than its melting point (Avérous, 2004). By the addition of water or
51 other plasticizers such as glycerol or sorbitol, the native crystalline structure of starch is
52 irreversibly disrupted (the so-called gelatinization phenomenon) and thus, the granular
53 starch is transformed into a thermoplastic starch (TPS) which vary from a soft material
54 (high plasticizer level) to a brittle material (low plasticizer level) depending on the
55 moisture and plasticizer level (Jiménez *et al.*, 2012).

56 The barrier to water vapor and oxygen are two essential properties to consider in starch-
57 based materials because oxygen and water molecules can deteriorate food properties.
58 Indeed, one of the main problems of starch-based films is their high water sensitivity
59 arising from their hydrophilic character, which leads to strong plasticization (Yan *et al.*,
60 2012). This effect negatively affects some characteristics such as the oxygen barrier
61 properties, which are excellent at low hydration levels and plasticizer content but
62 decrease as water sorption increases (Jiménez *et al.*, 2013, Yan *et al.*, 2012). Therefore,
63 many research works have focused on improving starch performance either by blending
64 it with other moisture resistant biodegradable polymers such as polylactic acid (PLA)
65 and polycaprolactone (PCL) (Ali Akbari Ghavimi *et al.*, 2015, Ayana *et al.*, 2014, Cai *et*
66 *al.*, 2014, Matzinos *et al.*, 2002, Ortega-Toro *et al.*, 2015) or through the addition of

1
2
3
4
5
6
7
8
9
10
11
12
13
14
15
16
17
18
19
20
21
22
23
24
25
26
27
28
29
30
31
32
33
34
35
36
37
38
39
40
41
42
43
44
45
46
47
48
49
50
51
52
53
54
55
56
57
58
59
60
61
62
63
64
65

67 dispersed nanoreinforcing agents to generate nanobiocomposites (Dean *et al.*, 2008,
68 Zeppa *et al.*, 2009). However, from an industrial implementation point of view, it is
69 important to highlight that complex multilayer structures are suggested as an alternative
70 to improve the performance of biopolymers, being the most efficient form to constitute
71 barrier materials (Fabra *et al.*, 2013, 2014). Whilst this multilayer design has been
72 widely used for synthetic materials, it has been scarcely developed for biodegradable
73 food packaging systems due to technological problems associated to the scaling-up
74 process and multilayer assembly. Nowadays, this methodology is being successfully
75 exploited by means of electrohydrodynamic processing, also known as electrospinning,
76 to improve the barrier and functional performance of biodegradable polymers
77 thermodynamically immiscible with the additional advantages of forming electrospun
78 coatings (Fabra *et al.*, 2014) or bioadhesives (Fabra *et al.*, 2015 ab) which show
79 excellent adhesion between layers, avoiding the use of synthetic adhesives.
80 Taking advantage of the methodology already described, this paper reports for the first
81 time, a comparative study in which the effect of different amounts of electrospun
82 biopolyesters coatings (polylactic acid –PLA-, polycaprolactone –PCL- and
83 polyhydroxybutyrate –PHB-) has been analyzed and compared in terms of barrier
84 efficiency.

85 86 **2. MATERIALS AND METHODS**

87 **2.1 Materials**

88 Polyhydroxybutyrate (PHB) pellets were supplied by Biomer (Krailling, Germany).
89 PHB was reported to have 0-40 wt% of plasticizers and an unreported amount of non-
90 toxic nucleating agents to improve melt processing (Hänggi, 2011). The semicrystalline
91 polylactide (PLA) used was a film extrusion grade produced by Natureworks (with a D-

1
2
3
4
5
6
7
8
9
10
11
12
13
14
15
16
17
18
19
20
21
22
23
24
25
26
27
28
29
30
31
32
33
34
35
36
37
38
39
40
41
42
43
44
45
46
47
48
49
50
51
52
53
54
55
56
57
58
59
60
61
62
63
64
65

92 isomer content of approximately 2%). The molecular weight had a number-average
93 molecular weight (Mn) of ca. 130,000 g/mol, and the weight average molecular weight
94 (Mw) was ca. 150,000 g/mol as reported by the manufacturer. The polycaprolactone
95 (PCL) grade FB100 was supplied by Solvay Chemicals (Belgium).

96 Corn starch (CS) was kindly supplied by Roquette (Roquette Laisa España, Benifaio,
97 Spain) and glycerol (Panreac Quimica, S.A. Castellar Del Vallés, Barcelona, Spain) was
98 used as plasticizer.

99 N,N-dimethylformamide (DMF) with 99% purity and trichloromethane (99% purity)
100 were purchased from Panreac Quimica S.A. (Barcelona, Spain). 2,2,2-Trifluoroethanol
101 (TFE) with 99% purity were purchased from Sigma-Aldrich (Spain). All products were
102 used as received without further purification.

103 104 **2.2. Preparation of films**

105 2.2.1 Preparation of thermoplastic corn starch films (TPCS)

106 Corn starch and glycerol, as plasticizer, were dispersed in water using a polymer:
107 glycerol: water ratio of 1:0.3:0.5 (w/w/w) and the dispersion was melt-mixed in a
108 Brabender Plastograph internal mixer at 130°C and 60 rpm for 4 minutes. The mixture
109 was then spread evenly on Teflon and placed in a compression mould (Carver 4122,
110 USA) at a pressure of 30000 lbs and 130°C for 5 minutes.

111 112 2.2.2 Preparation of multilayers TPCS systems

113 TPCS films were coated with PHB, PLA or PCL mats produced by means of the
114 electrospinning technique. PHB solutions in 2,2,2-trifluoroethanol having a total solids
115 content of 10 wt.% were used to generate the electrospun fibres. The PLA and PCL
116 electrospinning solutions were prepared by dissolving the required amount of the

1
2
3
4
5
6
7
8
9
10
11
12
13
14
15
16
17
18
19
20
21
22
23
24
25
26
27
28
29
30
31
32
33
34
35
36
37
38
39
40
41
42
43
44
45
46
47
48
49
50
51
52
53
54
55
56
57
58
59
60
61
62
63
64
65

117 biopolymer, under magnetic stirring, in a solvent prepared with a mixture of
118 trichloromethane (TCM):N,N-dimethylformamide (DMF) in order to reach a 5 or 12 %
119 in weight (wt.-%) of PLA and PCL, respectively. The TCM:DMF ratio used for PLA
120 and PCL was 85:15 and 65:35, respectively.

121 PHB, PLA or PCL fibre mats were directly electrospun onto both sides of the TPCS
122 films by means of a Fluidnatek® electrospinning pilot plant equipment from Bioinicia
123 S.L. (Valencia, Spain) equipped with a variable high-voltage 0-60 kV power supply.
124 Biopolyester solutions were electrospun under a steady flow-rate using a motorized high
125 throughput multinozzle injector, scanning vertically towards a metallic grid used as
126 collector, in which the neat TPCS film was attached. The distance between the needle
127 and the collector was 20, 24 and 31 cm for PHB, PLA and PCL, respectively, and the
128 experiments were carried out at ambient temperature. The voltage of the collector and
129 injector were set at 24 kV and 19 kV, respectively.

130 Different deposition times (0, 2, 10, 20, 40, 60 and 90 minutes), were evaluated in the
131 TPCS film to see how deposition time affected barrier properties. The total amount of
132 electrospun material (mg cm^{-1}) was estimated by weighing the TPCS film before and
133 after collection of the electrospun material.

134 With the aim of obtaining transparent and continuous outer layers based on PHB, PLA
135 or PCL, an additional heating step was applied. Coated TPCS films were placed
136 between hot plates at 160°C to melt and homogenize the PHB or PLA phase and 60°C to
137 melt the PCL layer.

138

139 **2.3. Characterization of films**

140

141 2.3.1. Scanning Electron Microscopy (SEM)

1
2
3
4
5
6
7
8
9
10
11
12
13
14
15
16
17
18
19
20
21
22
23
24
25
26
27
28
29
30
31
32
33
34
35
36
37
38
39
40
41
42
43
44
45
46
47
48
49
50
51
52
53
54
55
56
57
58
59
60
61
62
63
64
65

142 A Hitachi S-4800 microscope (Hitachi High Technology Corp., Tokyo, Japan) was used
143 to observe the morphology of films cross-sections. Cross-sections of the samples were
144 prepared by cryo-fracture of the films using liquid N₂. The samples were mounted on
145 bevel sample holders with double-sided adhesive tape, and sputtered with Au/Pd under
146 vacuum. Samples were observed using an accelerating voltage of 10 kV and a working
147 distance of 12–16 mm. Layer thicknesses were measured by means of the Adobe
148 Photoshop CS3 extended software from the SEM micrographs in their original
149 magnification.

151 2.3.3. Barrier properties

153 *2.3.3.1 Water Vapour Permeability (WVP)*

154 The WVP of TPCS and multilayer structures was determined by using the ASTM
155 (2011) gravimetric method using Payne permeability cups (Elcometer SPRL,
156 Hermelle/s Argenteau, Belgium) of 3.5 cm diameter. For each type of samples,
157 measurements were done in triplicate and water vapour permeability was carried out at
158 25°C and 0-100% relative humidity gradient, which was generated by using dry silica
159 gel and distilled water, respectively. The cups were weighed periodically (0.0001 g)
160 after the steady state was reached. Cups with aluminium films were used as control
161 samples to estimate solvent loss through the sealing. Water vapour permeation rate was
162 calculated from the steady-state permeation slopes (8 points) obtained from the
163 regression analysis of weight loss data vs. time, and weight loss was calculated as the
164 total cell loss minus the loss through the sealing. Permeability was obtained by
165 multiplying the permeance by the average film thickness.

166 Films thickness was measured in at least 5 different points using a digital micrometer
167 (Mitutoyo, Spain) with ± 0.001 mm accuracy.

168

169 *2.3.3.2 Oxygen permeability (O_2P)*

170 The O_2P was derived from oxygen transmission rate (OTR) measurements recorded, in
171 triplicate, using an Oxygen Permeation Analyzer M8001 (Systech Illinois, UK) at 80%
172 RH and 23°C. A sample of each multilayer film (5 cm²) was placed in the test cell and
173 pneumatically clamped in place. The samples were previously purged with nitrogen in
174 the humidity equilibrated samples, before exposure to an oxygen flow of 10 mL min⁻¹.
175 In order to obtain the oxygen permeability, film thickness was considered in each case.

176

177 *2.3.4. Contact Angle Measurements*

178 Measurements of contact angle were performed at room conditions (*ca.* 23°C and 53%
179 RH) in a Video-Based Contact Angle Meter model OCA 20 (Data Physics Instruments
180 GmbH, Filderstadt, Germany). Data were obtained by analysing the shape of a distilled
181 water drop after it had been placed over the film for 5 s. Image analyses were carried
182 out by SCA20 software. At least, eight replicates were made for each sample.

183

184 **2.4. Statistical Analysis**

185 Statistical analysis was performed using the analysis of variance procedure (ANOVA)
186 with StatGraphics Plus version 5.1 (Statistical Graphics Corp.). Fisher's Least
187 Significant Difference (LSD) test was applied to detect differences of means, and
188 $p < 0.05$ (95% significant level) was considered to be statistically significant.

189

190

1
2
3
4
5
6
7
8
9
10
11
12
13
14
15
16
17
18
19
20
21
22
23
24
25
26
27
28
29
30
31
32
33
34
35
36
37
38
39
40
41
42
43
44
45
46
47
48
49
50
51
52
53
54
55
56
57
58
59
60
61
62
63
64
65

191 3. RESULTS AND DISCUSSION

192 3.2 Microstructure of multilayer films

193 Since it is well-known that barrier properties of biopolymers are strongly related to their
194 morphology, SEM was used to evaluate the films' homogeneity, layer structure,
195 presence of pores and cracks, surface smoothness and thickness. SEM micrographs of
196 the surface images of the multilayer TPCS-based films are shown in Figure 1. TPCS
197 film presented homogeneous and smooth surfaces, without visible pores and cracks (see
198 Figure 1). Besides, it was clearly observed that annealing the PCL, PLA and PHB fibres
199 favoured the formation of a continuous coating layer which could contribute to improve
200 the barrier properties of the TPCS films.

201 The cross-section image of the TPCS film showed a compacted structure with absence
202 of intact starch granules, demonstrating the effectiveness of the destructure and
203 thermo-compression processes (*cf.* Figure 2A). Representative images of the multilayer
204 structures prepared with PCL, PLA or PHB are shown in Figures 2, 3 and 4,
205 respectively. The first clear observation of these multilayer films was that all samples
206 exhibited a laminate-like structure in which relatively homogeneous biopolyester
207 coatings were formed onto both sides of the TPCS films. Furthermore, the adhesion
208 between the outer layers and the TPCS film was very good and only a weak
209 delamination occurred after cryo-fracturing the material in some of the samples.

210 From the cross-section micrographs, it is also interesting to note that the thickness of the
211 outer layer depended on the biopolyester used and thus, on the electrospinning solutions
212 and the morphology of the electrospun fibres. Therefore, the amount of the coating layer
213 was estimated by weighting the TPCS before and after the electrospinning process and
214 it was observed that, for a given amount of the electrospun layer, the thickness of the
215 coating was governed by the polymer concentration used in the electrospinning solution

1
2
3
4
5
6
7
8
9
10
11
12
13
14
15
16
17
18
19
20
21
22
23
24
25
26
27
28
29
30
31
32
33
34
35
36
37
38
39
40
41
42
43
44
45
46
47
48
49
50
51
52
53
54
55
56
57
58
59
60
61
62
63
64
65

216 and the diameter of the electrospun fibres (Pérez-Masiá *et al.*, 2013; Chalco-Sandoval *et*
217 *al.*, 2014). A lineal relationship was observed between the thickness and the deposited
218 amount of the electrospun coating, as it will be detailed below (see Figure 5). In this
219 sense, for a given amount of the electrospun layer (*i.e.* 5 mg·cm⁻²), PHB provided
220 thicker layers and PLA the thinnest ones. As it was previously reported by Pérez-Masiá
221 *et al.*, 2013, PLA fibres were thinner than those obtained for PCL and PHB, in identical
222 electrospinning conditions as the ones applied in the present work. Therefore, after the
223 annealing process, PLA fibres were better compacted than PCL and PHB thus providing
224 thinner layers. Besides, when comparing the thicker ones (PCL and PHB), an excellent
225 interfacial adhesion between PCL and thermoplastic starch (TPS) melt phases have been
226 reported elsewhere (Ortega-Toro *et al.*, 2015, Cai *et al.*, 2014) in composite PCL/TPS
227 films which could also contribute to the increased attractive forces through hydrogen
228 bonding interactions between the ester carbonyl of PCL and the –OH groups of starch,
229 thus, reducing the thickness of the outer PCL layers when compared to the PHB layer
230 thickness. This interaction could lead to lowering the interfacial tension between both
231 materials, leading to compatibilization (Cai *et al.*, 2014). This could also explain the
232 good adhesion between PCL and TPCS layers.

233 234 **3.3 Barrier properties**

235 Figures 5 and 6 show the water vapour (WVP) and oxygen permeability (O₂P) values of
236 the neat TPCS films and the developed multilayer structures. Water and oxygen barrier
237 properties of the uncoated TPCS films developed in this work were in the same order as
238 those reported in the literature for films prepared by melt-compounding (Ortega-Toro *et*
239 *al.*, 2015). However, comparing with the literature data, these films were less permeable
240 than their counterparts prepared by solvent casting (Jiménez *et al.*, 2012; Müller *et al.*,

2011, Pushpadas *et al.*, 2008). Thus, one can firstly conclude that the processing method used during film-formation played an important role in the final properties of the films. This can be ascribed to the fact that the casting process involved long drying times which contributed to the formation of a more open microstructure due to the solvent evaporation phenomenon, creating channels throughout which water molecules could easily diffuse. However, using the compression-moulding method, polymer chains were more compacted giving rise to a denser structure. A similar trend was observed comparing other biopolymer matrices such as PHA (Fabra *et al.*, 2013) or PLA (Byun, Kim and Whiteside, 2010; Rhim, Hong, and Ha, 2009; Sánchez-García and Lagaron, 2010ab).

Figure 5 displays the water vapour permeability values of the developed multilayer structures. As mentioned on above, the thickness of the outer layers linearly increased as the mg (PCL, PLA or PHB) $\cdot\text{cm}^{-2}$ increased, whatever the biopolyester used. Interestingly, the WVP values decreased exponentially as the mg coating layer $\cdot\text{cm}^{-2}$ increased ($y=b\cdot e^{ax}$). However, PHB was more efficient in reducing water vapour permeability of TPCS films than PCL and PLA biopolymers. This agrees with the greater water vapour permeability values of the neat PLA and PCL films (1.2 and 1.4 kg $\text{Pa}^{-1} \text{m}^{-2} \text{s}^{-1}$, for PLA and PCL respectively) (Ambrosio-Martin *et al.*, 2014; Bychuk, Kil'deeva and Cherdyntseva, 2014) as compared to the WVP obtained for a neat PHB film (0.16 kg $\text{Pa}^{-1} \text{m}^{-2} \text{s}^{-1}$) (Plackett and Siró, 2011). Coefficients a , b and R^2 are given in Table 1. The greater barrier efficiency on TPCS films is reflected through the lower a and b values. Due to the abrupt permeability decrease for the multilayer structures prepared with PHB as compared to the neat TPCS film, the regression coefficient from the exponential model considering the whole mg PHB $\cdot\text{cm}^{-2}$ range was only ~ 0.93 , so another fit only considering data of multilayer samples (without taking into account the

1
2
3
4
5
6
7
8
9
10
11
12
13
14
15
16
17
18
19
20
21
22
23
24
25
26
27
28
29
30
31
32
33
34
35
36
37
38
39
40
41
42
43
44
45
46
47
48
49
50
51
52
53
54
55
56
57
58
59
60
61
62
63
64
65

266 permeability of the neat TPCS film) was carried out, which allowed us to make better
267 predictions. The obtained values indicate that it is possible to use smaller amounts of
268 PHB electrospun outer layer than PLA or PCL to achieve the same barrier efficiency.
269 Concretely, for a given amount of electrospun coating (i.e. $5 \text{ mg} \cdot \text{cm}^{-2}$), the WVP of
270 TPCS films dropped down to *ca.* 83, 88 and 91% for PCL, PLA and PHB multilayer
271 structures, respectively. Accordingly, the greatest reduction was observed when coating
272 the TPCS film with the greatest amount (expressed as $\text{mg} \cdot \text{cm}^{-2}$) of electrospun PHB
273 fibres, where the WVP dropped down to *ca.* 99 %.

274 A similar trend was observed for oxygen barrier properties, measured at 80% RH (*cf.*
275 Figure 6). The total amount of electrospun coating was also exponentially related with
276 oxygen barrier properties, being the PHB the biopolyester which provided the greatest
277 reduction in O_2P values. The coefficients a , b and R^2 of the fitting model are given in
278 Table 2. Once again, the greater barrier efficiency on TPCS films was evidenced by the
279 lower b values found for the multilayer structures prepared with PHB. In fact, for a
280 given amount of electrospun coating (*i.e.* $5 \text{ mg} \cdot \text{cm}^{-2}$), the oxygen permeability of
281 multilayer structures was improved up to $\sim 91\%$ for PLA and PCL and $\sim 95\%$ for PHB
282 as compared to the neat TPCS film. For oxygen barrier, the exponential model was also
283 reported considering only the data of PLA and PHB multilayer structures (without the
284 neat TPCS film), which allowed to make better predictions.

285 Thus, barrier results highlighted the suitability of this methodology to develop fully
286 biodegradable multilayer structures with improved barrier performance which could be
287 adapted depending on the final intended used.

289 **3.4 Contact angle**

1
2
3
4
5
6
7
8
9
10
11
12
13
14
15
16
17
18
19
20
21
22
23
24
25
26
27
28
29
30
31
32
33
34
35
36
37
38
39
40
41
42
43
44
45
46
47
48
49
50
51
52
53
54
55
56
57
58
59
60
61
62
63
64
65

290 The wettability properties of the TPCS films and the coated multilayer structures were
291 determined by direct measurement of contact angles of a water drop deposited on the
292 upper surface of the samples in order to investigate the effect of the PCL, PLA and PHB
293 coating layers on the surface water affinity. Contact angle was measured for the neat
294 TPCS and for multilayer structures prepared with the lowest and highest deposition
295 times. Since the deposition time did not match with the amount of biopolyester
296 deposited onto each side of the TPCS film, contact angle of multilayer structures
297 prepared with $3.2 \text{ mg}\cdot\text{cm}^{-2}$ electrospun coatings were also measured for comparative
298 purposes. The results are displayed in Table 3 and Figure 7, showing that all of them
299 (PCL, PLA and PHB) were quite effective in protecting the TPCS inner layer from
300 moisture. It might be noted that the resulted contact angle values of the developed
301 multilayer structures were in the same range as for the neat PLA and PCL biopolymers
302 (de Campos *et al.*, 2013; Chan *et al.*, 2013; Darie *et al.*, 2014) although lower to contact
303 angles reported in the literature for neat PHB films (Zhijiang *et al.*, 2016). This
304 difference could be ascribed to the intrinsic plasticizer content in the original PHB
305 pellets. As mentioned before, PHB was originally reported to have between 0 and 40
306 wt% plasticizer in order to improve melt processing (Hänggi, 2011).

307 308 **4. CONCLUSIONS**

309 Multilayer technology is a common and efficient technique used to improve the
310 physicochemical properties, mainly barrier, of the hydrophilic materials. In this work,
311 TPCS multilayer systems containing electrospun biopolyester outer layers based on PCL,
312 PLA or PHB have been developed. The incorporation of electrospun biopolyester
313 coating layers effectively improved water vapour and oxygen barrier properties of the

1
2
3
4
5
6
7
8
9
10
11
12
13
14
15
16
17
18
19
20
21
22
23
24
25
26
27
28
29
30
31
32
33
34
35
36
37
38
39
40
41
42
43
44
45
46
47
48
49
50
51
52
53
54
55
56
57
58
59
60
61
62
63
64
65

314 TPCS films, although the PHB was the most efficient in reducing both water and
315 oxygen permeability values.

316

317 **Acknowledgments**

318 The authors acknowledge financial support from MINECO (AGL2015-63855-C2-1).
319 M. J. Fabra is recipient of a Ramon y Cajal contract (RYC-2014-158) from the Spanish
320 Ministry of Economy and Competitiveness, respectively.

321

322 **REFERENCES**

323 Ali Akbari Ghavimi, S., Ebrahimzadeh, M.H., Solati-Hashjin, M., Abu Osman, N.A.
324 (2015). Polycaprolactone/starch composite: Fabrication, structure, properties, and
325 applications. *Journal of Biomedical Materials Research - Part A*, 103 (7), 2482-2498
326 Ambrosio-Martín, J., Fabra, M.J., Lopez-Rubio, A., and Lagaron, J.M. (2014). An
327 effect of lactic acid oligomers on the barrier properties of polylactide. *Journal of*
328 *Material Science*, 49(8), 2975-2986.
329 ASTM, 1995. Standard test methods for water vapour transmission of materials.
330 Standards designations: E96-95. In: Annual Book of ASTM Standards. *American*
331 *Society for Testing and Materials*, Philadelphia, PA, pp. 406-413.
332 Averous L. (2004). Biodegradable multiphase systems based on plasticized starch: A
333 review. *J Macromol Sci-Pol R*, 3:231-274.
334 Ayana, B., Suin, S., Khatua, B.B. (2014). Highly exfoliated eco-friendly thermoplastic
335 starch (TPS)/poly (lactic acid)(PLA)/clay nanocomposites using unmodified nanoclay.
336 *Carbohydrate Polymers*, 110, 430-439.

- 1
2
3
4
5
6
7
8
9
10
11
12
13
14
15
16
17
18
19
20
21
22
23
24
25
26
27
28
29
30
31
32
33
34
35
36
37
38
39
40
41
42
43
44
45
46
47
48
49
50
51
52
53
54
55
56
57
58
59
60
61
62
63
64
65
- 337 Bychuk, M.A., Kil'deeva, N.R., Cherdyntseva, T.A. (2014). Films of a biodegradable
338 polyester mixture with antimicrobial and proteolytic activity. *Pharmaceutical Chemistry*
339 *Journal*, 48 (1), 60-64.
- 340 Byun, Y., Kim, Y. T., and Whiteside, S. (2010). Characterization of an antioxidant
341 polylactic acid (PLA) film prepared with α -tocopherol, BHT and polyethylene glycol
342 using film cast extruder. *Journal of Food Engineering*, 100, 239-244.
- 343 Cai, J., Xiong, Z., Zhou, M., Tan, J., Zeng, F., Ma, M., Lin, S. and Xiong, H. (2014).
344 Thermal properties and crystallization behavior of thermoplastic starch/poly(ϵ -
345 caprolactone) composites. *Carbohydrate Polymers*, 102, 746-754.
- 346 Chan, R.T.H, Marçal, H., Ahmed, T., Russel, R.A., Holden, P.J., and Foster, L.J.R.
347 (2013). Poly(ethylene glycol)-modulated cellular biocompatibility of
348 polyhydroxyalkanoate films. *Polymer International*, 62, 884-892.
- 349 Chalco-Sandoval, W., Fabra, M.J., Lopez-Rubio, A., Lagaron, J.M. (2014). Electrospun
350 heat management polymeric materials of interest in food refrigeration and packaging.
351 *Journal of Applied Polymer Science*, 131 (1) 40661.
- 352 Darie, R.M., Pâslaru, E., Sdrobis, A., Pricope, G.M., Hitruc, G.E., Poiata, A.,
353 Baklavaridis, A. and Vasile, C. (2014). Effect of Nanoclay Hydrophilicity on the
354 Poly(lactic acid)/Clay Nanocomposites Properties. *Industrial and Engineering*
355 *Chemistry Research*, 7877-7890.
- 356 Dean, K.M., Do, M. D., Petinakis, E. and Yu, L. (2008): Key interactions in
357 biodegradable thermoplastic starch/poly(vinyl alcohol)/montmorillonite micro- and
358 nanocomposites. *Composite Science and Technology*, 68, 1453-1462.
- 359 de Campos, A., Tonoli, G.H.D., Marconcini, J.M., MAttoso, L.H.C., Klamczynski, A.,
360 Gregorski, K.S., Wood, D., Williams, T., Chiou, B.-S., Imam, S.H. (2013). TPS/PCL

1
2
3
4
5
6
7
8
9
10
11
12
13
14
15
16
17
18
19
20
21
22
23
24
25
26
27
28
29
30
31
32
33
34
35
36
37
38
39
40
41
42
43
44
45
46
47
48
49
50
51
52
53
54
55
56
57
58
59
60
61
62
63
64
65

361 Composite Reinforced with Treated Sisal Fibers: Property, Biodegradation and Water-
362 Absorption. *Journal of Polymers and the Environment*, 21, 1-7

363 Fabra, M.J., López-Rubio, A., and Lagaron, J.M. (2013). High barrier
364 polyhydroxyalkanoate food packaging film by means of nanostructured electrospun
365 interlayers of zein. *Food Hydrocolloids*, 32, 106-114.

366 Fabra, M.J., López-Rubio, A. and Lagaron, J.M. (2014). Nanostructured interlayers of
367 zein to improve the barrier properties of high barrier polyhydroxyalkanoates and other
368 polyesters. *Journal of Food Engineering*, 127, 1-9.

369 Fabra, M.J., López-Rubio, A. and Lagaron, J.M. (2015a). Effect of the film-processing
370 conditions, relative humidity and aging on wheat gluten films coated with electrospun
371 polyhydroxyalkanoate. *Food Hydrocolloids*, 44, 292-299.

372 Fabra, M.J., López-Rubio, A. and Lagaron, J.M. (2015b). Three-Layer Films Based on
373 Wheat Gluten and Electrospun PHA. *Food and Bioprocess Technology*, 8(11), 2330-
374 2340.

375 Hänggi, U. J. (2011). Biomer biopolyesters. Germany: Krailling.

376 Hutchings, J. B. (1999). Food and colour appearance (2nd ed.). Gaithersburg,
377 M.D.:Chapman and Hall Food Science Book, Aspen Publication.

378 Jiménez, A., Fabra, M.J., Talens, P. and Chiralt, A. (2012). Edible and Biodegradable
379 Starch Films: A Review. *Food and Bioprocess Technology*, 5(6), 2058-2076.

380 Jiménez, A., Fabra, M.J., Talens, P. and Chiralt, A. (2013). Phase transitions in starch
381 based films containing fatty acids. Effect on water sorption and mechanical behaviour.
382 *Food Hydrocolloids*, 30 (1), 408-418.

383 Matzinos P, Tserki V, Kontoyiannis A, Panayiotou C. (2002). Processing and
384 characterization of starch/polycaprolactone products. *Polymer Degradation and
385 Stability*, 1, 17-24.

1
2
3
4
5
6
7
8
9
10
11
12
13
14
15
16
17
18
19
20
21
22
23
24
25
26
27
28
29
30
31
32
33
34
35
36
37
38
39
40
41
42
43
44
45
46
47
48
49
50
51
52
53
54
55
56
57
58
59
60
61
62
63
64
65

386 Müller, C. M. O., Laurindo, J. B., and Yamashita. (2011). Effect of nanoclay
387 incorporation method on mechanical and water vapor barrier properties of starch-based
388 films. *Industrial Crops and Products*, 33, 605–610.

389 Ortega-Toro, R., Contreras, J., Talens, P., Chiralt., A. (2015). Physical and structural
390 properties and thermal behaviour of starch-poly(ϵ -caprolactone) blend films for
391 food packaging . *Food Packaging and Shelf Life*, 5, 10-20.

392 Pérez-Masiá, R., López-Rubio, A., Fabra, M.J., and Lagaron, J.M. (2013).
393 Biodegradable Polyester-Based Heat Management Materials of Interest in Refrigeration
394 and Smart Packaging Coatings. *Journal of Applied Polymer Science*, 30(5), 3251-3262.

395 Plackett, D., and Siro, I. (2011). Polyhydroxyalkanoates (PHAs) for food packaging. In
396 J. M. Lagaron (Ed.), *Multifunctional and nanoreinforced polymers for food packaging*.
397 Cambridge. UK: Woodhead Publishing Limited.

398 Pushpadass, H. A., Marx, D. B., and Hanna, M. A. (2008). Effects of extrusion
399 temperature and plasticizers on the physical and functional properties of starch films.
400 *Starch/Stärke*, 60, 527–538.

401 Rhim, J. W., Hong, S. I., and Ha, C. S. (2009). Tensile, water vapor barrier and
402 antimicrobial properties of PLA/nanoclay composite films. *LWT - Food Science and*
403 *Technology*, 42, 612-617.

404 Sánchez-García, M. D., and Lagaron, J. M. (2010a). On the use of plant cellulose
405 nanowhiskers to enhance the barrier properties of polylactic acid. *Cellulose*, 17, 987-
406 1004.

407 Sánchez-García, M. D., and Lagaron, J. M. (2010b). Novel Clay-Based
408 Nanobiocomposites of Biopolyesters with Synergistic Barrier to UV Light, Gas, and
409 Vapour. *Journal of Applied Polymer Science*, 118, 188–199.

1
2
3
4
5
6
7
8
9
10
11
12
13
14
15
16
17
18
19
20
21
22
23
24
25
26
27
28
29
30
31
32
33
34
35
36
37
38
39
40
41
42
43
44
45
46
47
48
49
50
51
52
53
54
55
56
57
58
59
60
61
62
63
64
65

410 Xu, Y. X., Kimb, K. M., Hanna, M. A., and Nag, D. (2005). Chitosan starch composite
411 film: preparation and characterization. *Industrial Crops and Products*, 21(2), 185-192.
412 Yan, Q., Hou, H., Guo, P., Dong, H., 2012. Effects of extrusion and glycerol content on
413 properties of oxidized and acetylated corn starch-based films. *Carbohydrate Polymers*,
414 87 (1), 707–712.
415 Zhijiang, C., Yi, X., Haizheng, Y., Jia, J., Liu, Y. (2016).
416 Poly(hydroxybutyrate)/cellulose acetate blend nanofiber scaffolds: Preparation,
417 characterization and cytocompatibility. *Materials Science and Engineering C*, 58, 5760,
418 757-767.
419
420
421

422 **Table 1.** Values of a , b coefficients and R^2 in the relationship between WVP
 423 and mg (PCL, PLA or PHB) · cm⁻²

Coating layer	Model	-a	b	R ²
PCL	exponential	0.478	4.00E-17	0.992
PLA		0.413	3.00E-17	0.928
without TPCS		0.351	2.00E-17	0.983
PHB		0.425	2.00E-17	0.936
without TPCS		0.378	1.00E-17	0.947

424
 425 **Table 2.** Values of a , b coefficients and R^2 in the relationship between O₂P
 426 and mg (PCL, PLA or PHB) · cm⁻²

Coating layer	Model	-a	b	R ²
PCL	exponential	0.478	4.00E-17	0.992
PLA		0.413	3.00E-17	0.928
without TPCS		0.351	2.00E-17	0.983
PHB		0.425	2.00E-17	0.936
without TPCS		0.378	1.00E-17	0.947

427
 428 **Table 3.** Contact angle values of the neat thermoplastic corn starch-based films, the
 429 developed multilayer structures and the neat PHB, PLA and PCL films.

Coating layer	mg · cm ⁻²	θ (°)
		54.8 (3.5) ^a
PCL	0.8	82.2 (2.5) ^b
	3.2	81.9 (3.0) ^b
	7	78.5 (4.4) ^b
PLA	0.5	84.0 (3.8) ^b
	3.2	84.1 (2.6) ^b
	4.9	83.2 (3.6) ^b
PHB	1.5	81.6 (2.6) ^b
	3.2	84.2 (2.4) ^b
	13.6	86.5 (3.1) ^b
PHB		123 (3.5) ^(*)
PLA		86.9 (1.6) ^(**)
PCL		89.5 (1.9) ^(***)

430 ^(*)Zhijiang *et al.*, 2016 ^(**)Darie *et al.*, 2014 ^(***)Campos *et al.*, 2008
 431 a-b: Different superscripts within the same column indicate significant differences among samples ($p < 0.05$).
 432

433 **Figure captions**

1
2 434 **Figure 1.** Surface images of the neat TPCS film (A) and the developed multilayer films
3 prepared with PCL (B), PLA (C) or PHB (D).
4
5

6
7 436 **Figure 2.** Cross-section images of the neat TPCS and multilayer films prepared with
8 PCL at different deposition times (A) TPCS, (B) 20 min, (C) 40 min and (D) 90 min.
9
10 437

11 438 **Figure 3.** Cross-section images of the multilayer films prepared with PLA at different
12 deposition times (A) 2 min, (B) 20 min, (C) 40 min and (D) 60 min.
13
14 439

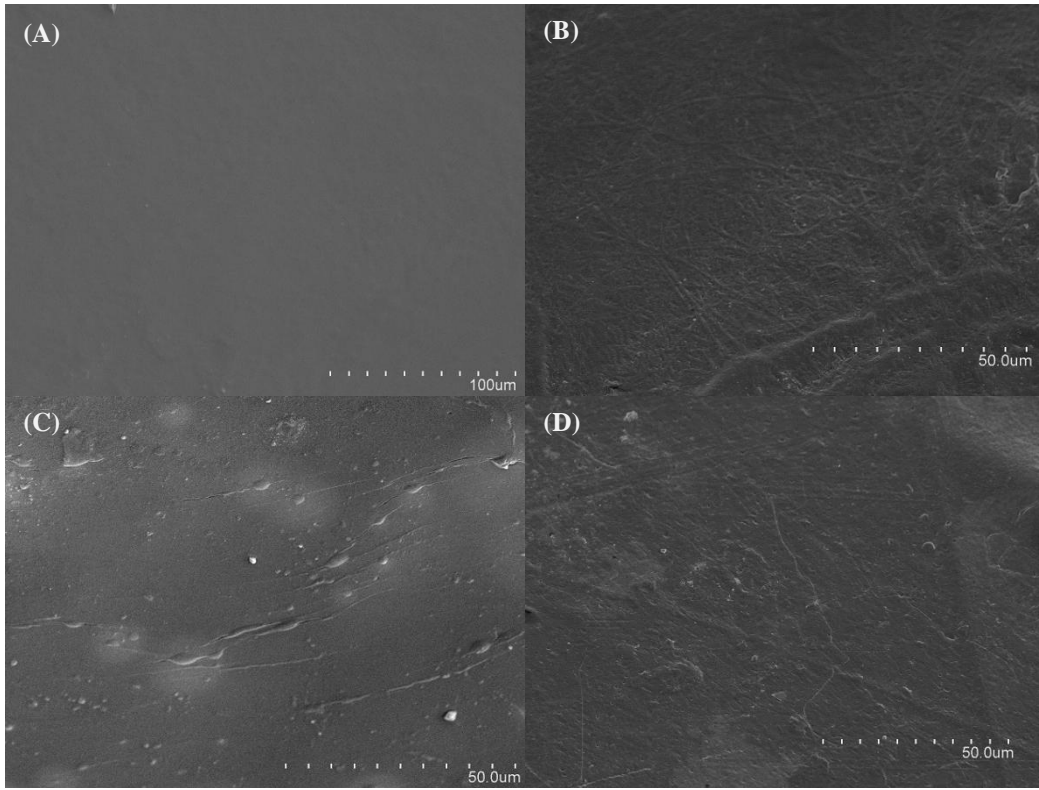
15
16 440 **Figure 4.** Cross-section images of the multilayer films prepared with PHB at different
17 deposition times (A) 20min, (B) 40 min, (C) 60 min and (D) 90 min.
18
19 441

20
21 442 **Figure 5.** Relationships between WVP values *vs.* the mg electrospun coating $\cdot \text{cm}^2$ and
22 thickness *vs.* the mg electrospun coating $\cdot \text{cm}^2$
23
24 443

25
26 444 **Figure 6.** Relationships between O_2P values *vs.* the mg electrospun coating $\cdot \text{cm}^2$ and
27 thickness *vs.* the mg electrospun coating $\cdot \text{cm}^2$
28
29 445

30
31 446 **Figure 7.** Images of water droplet in contact angle measurements of the uncoated TPCS
32 film (A) and the developed multilayer films prepared with the highest deposited amount
33 of PCL (B), PLA (C) or PHB (D).
34
35 447
36
37 448
38
39
40
41
42
43
44
45
46
47
48
49
50
51
52
53
54
55
56
57
58
59
60
61
62
63
64
65

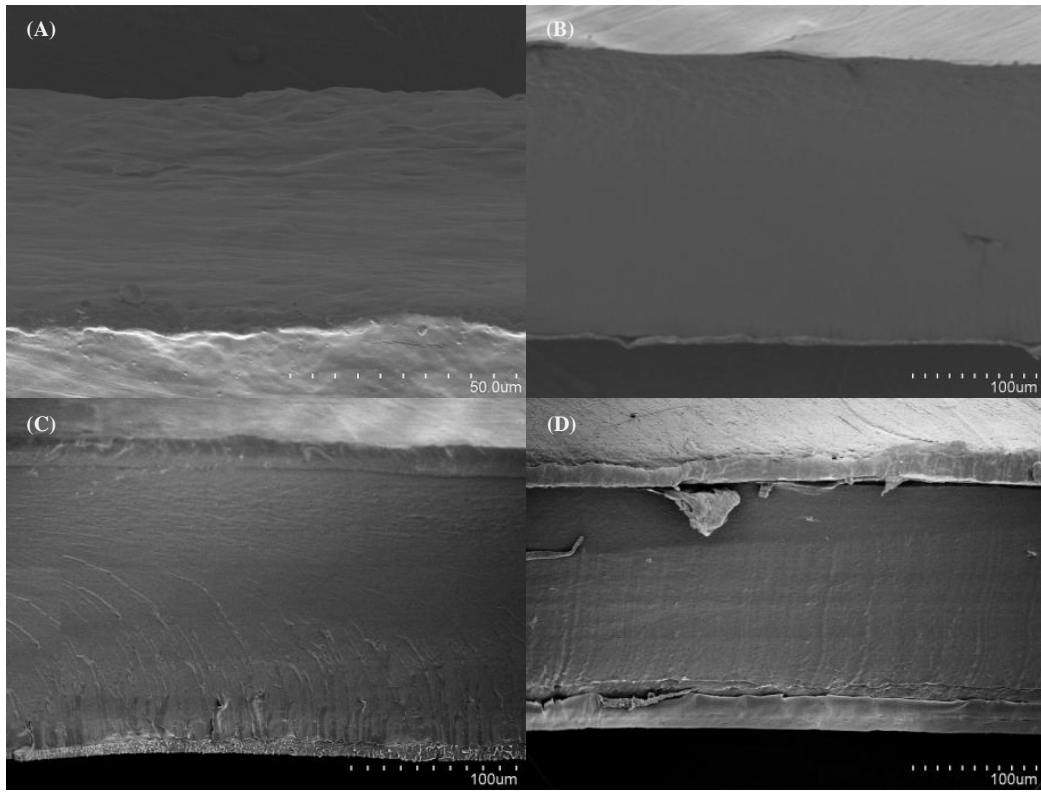
449 **Figure 1**



450

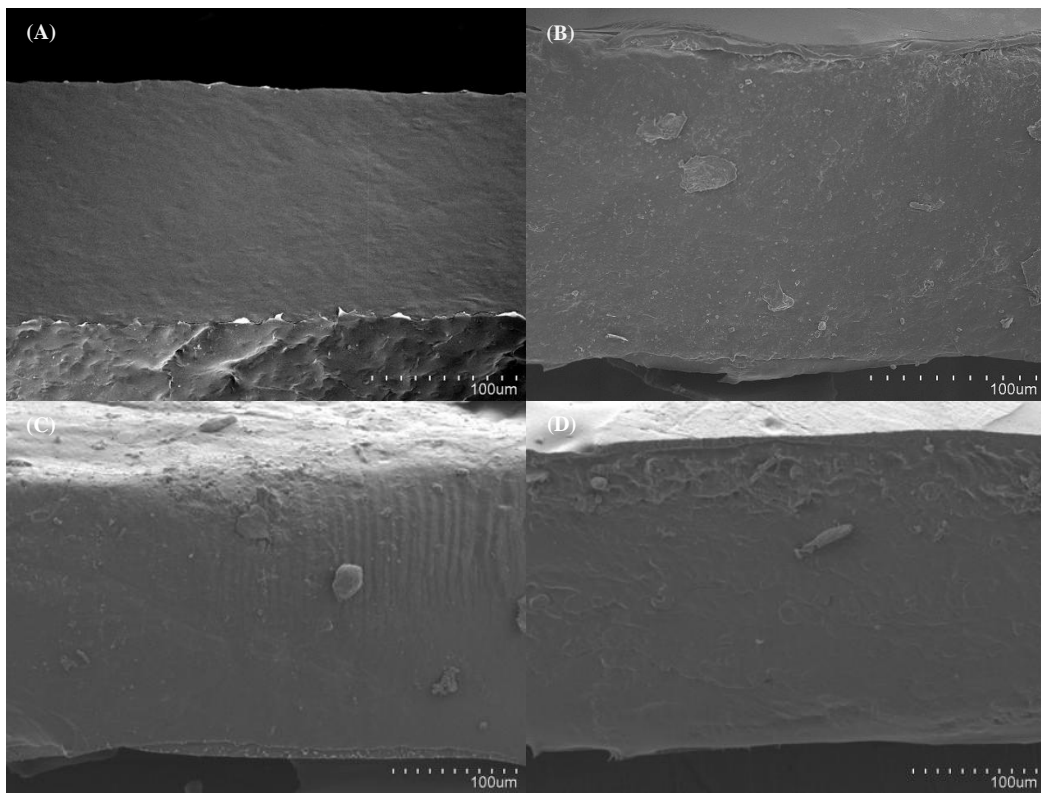
1
2
3
4
5
6
7
8
9
10
11
12
13
14
15
16
17
18
19
20
21
22
23
24
25
26
27
28
29
30
31
32
33
34
35
36
37
38
39
40
41
42
43
44
45
46
47
48
49
50
51
52
53
54
55
56
57
58
59
60
61
62
63
64
65

451 **Figure 2**



452

453 **Figure 3**

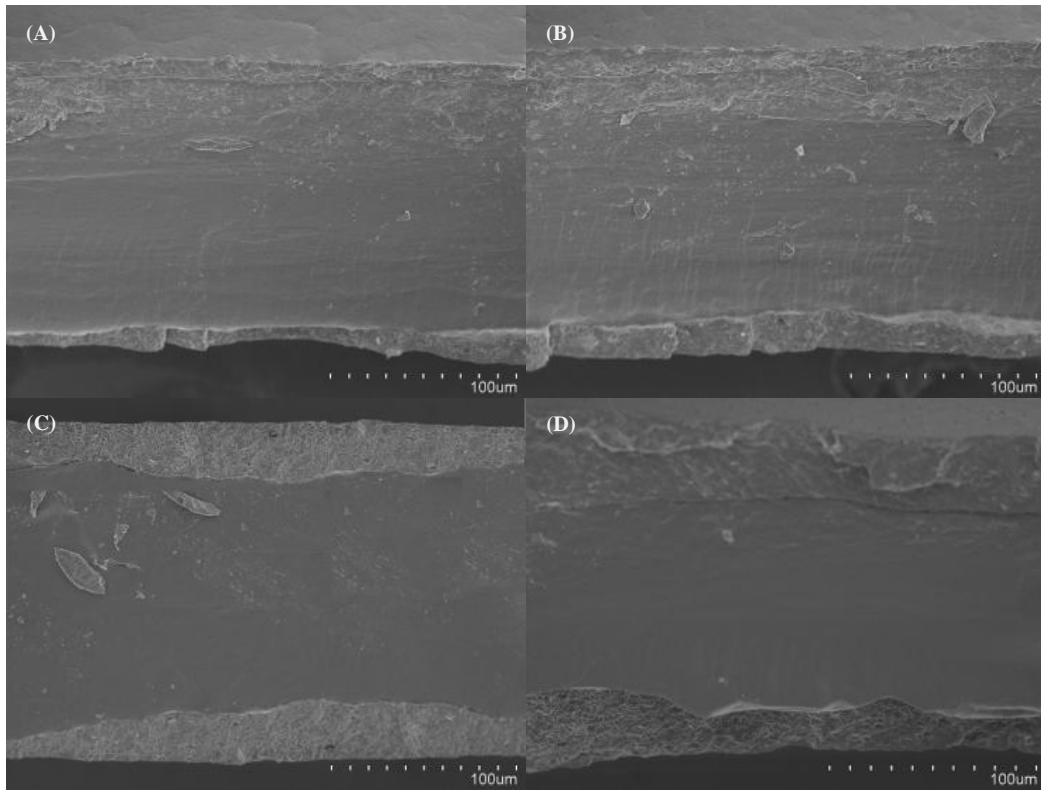


454

455

1
2
3
4
5
6
7
8
9
10
11
12
13
14
15
16
17
18
19
20
21
22
23
24
25
26
27
28
29
30
31
32
33
34
35
36
37
38
39
40
41
42
43
44
45
46
47
48
49
50
51
52
53
54
55
56
57
58
59
60
61
62
63
64
65

456 **Figure 4**



1
2
3
4
5
6
7
8
9
10
11
12
13
14
15
16
17
18
19
20
21
22
23
24
25
26
27
28
29
30
31
32
33
34
35
36
37
38
39
40
41
42
43
44
45
46
47
48
49
50
51
52
53
54
55
56
57
58
59
60
61
62
63
64
65

457

458

459

460

461

462

463

464

465

466

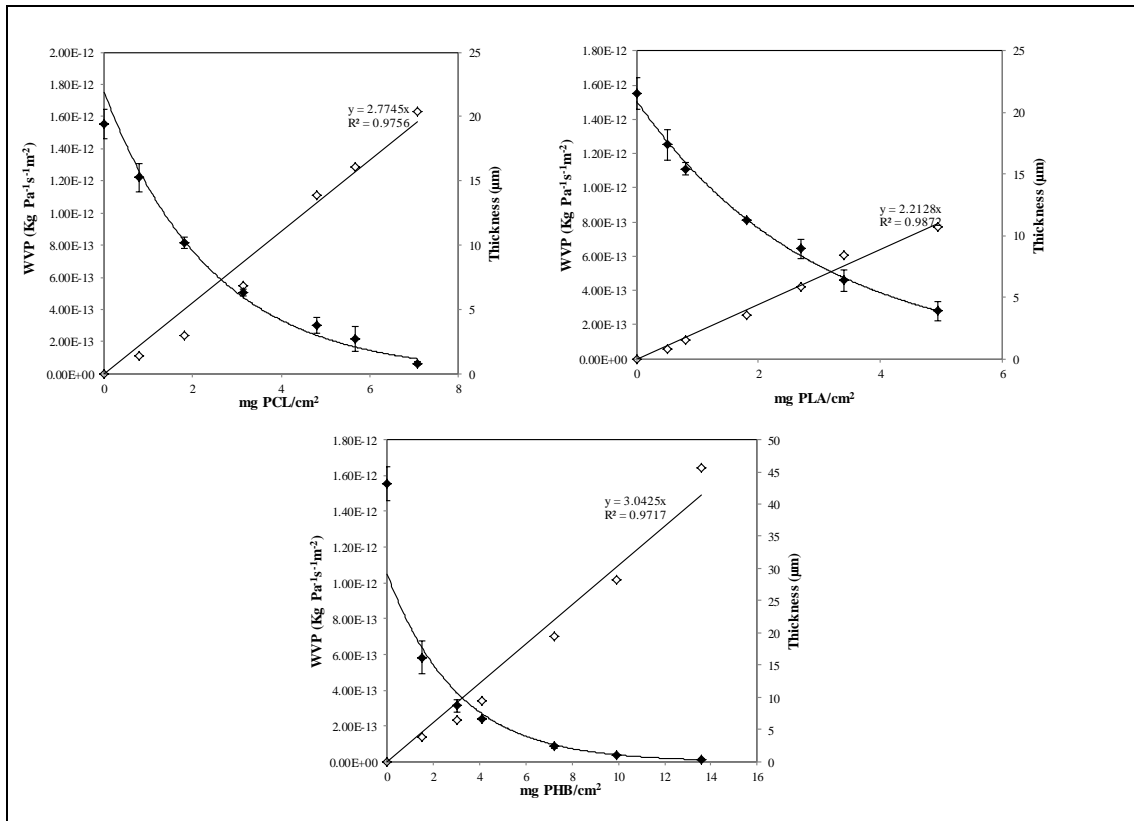
467

468

469

470

471 **Figure 5**

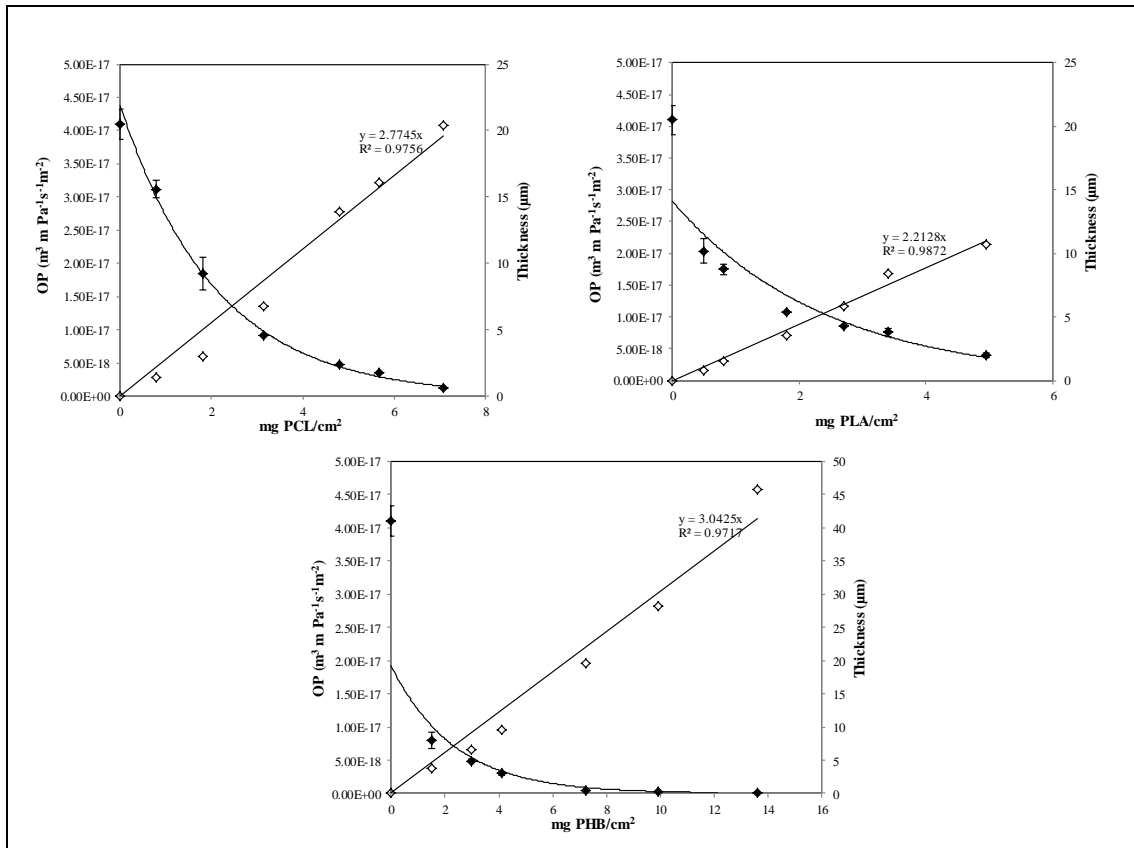


472

473

1
2
3
4
5
6
7
8
9
10
11
12
13
14
15
16
17
18
19
20
21
22
23
24
25
26
27
28
29
30
31
32
33
34
35
36
37
38
39
40
41
42
43
44
45
46
47
48
49
50
51
52
53
54
55
56
57
58
59
60
61
62
63
64
65

474 **Figure 6**

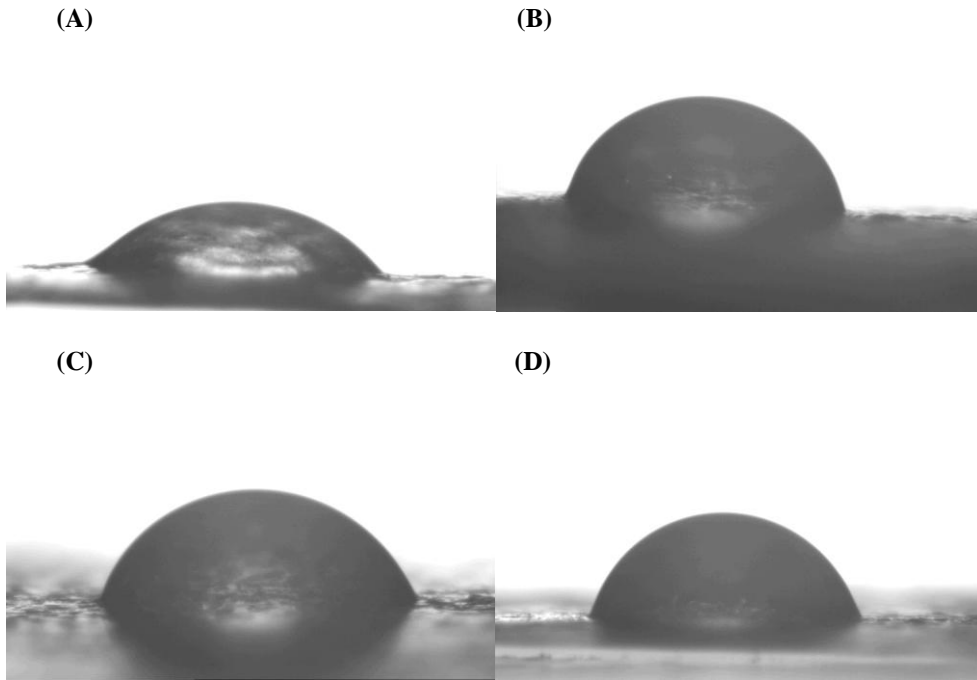


475

476

1
2
3
4
5
6
7
8
9
10
11
12
13
14
15
16
17
18
19
20
21
22
23
24
25
26
27
28
29
30
31
32
33
34
35
36
37
38
39
40
41
42
43
44
45
46
47
48
49
50
51
52
53
54
55
56
57
58
59
60
61
62
63
64
65

477 **Figure 7**



478

479

1
2
3
4
5
6
7
8
9
10
11
12
13
14
15
16
17
18
19
20
21
22
23
24
25
26
27
28
29
30
31
32
33
34
35
36
37
38
39
40
41
42
43
44
45
46
47
48
49
50
51
52
53
54
55
56
57
58
59
60
61
62
63
64
65